THE APPLICATION OF INFRARED THERMOGRAPHIC INSPECTION TECHNIQUES TO THE SPACE SHUTTLE THERMAL PROTECTION SYSTEM

K. E. Cramer and W. P. Winfree

NASA, Langley Research Center, 3b East Taylor St., Mail Stop 231, Hampton, VA 23681, USA
k.e.cramer@nasa.gov

The Nondestructive Evaluation Sciences Branch at NASA's Langley Research Center has been actively involved in the development of thermographic inspection techniques for more than 15 years. Since the Space Shuttle *Columbia* accident, NASA has focused on the improvement of advanced NDE techniques for the Reinforced Carbon-Carbon (RCC) panels that comprise the orbiter's wing leading edge. Various nondestructive inspection techniques have been used in the examination of the RCC, but thermography has emerged as an effective inspection alternative to more traditional methods. Thermography is a non-contact inspection method as compared to ultrasonic techniques which typically require the use of a coupling medium between the transducer and material. Like radiographic techniques, thermography can be used to inspect large areas, but has the advantage of minimal safety concerns and the ability for single-sided measurements.

Principal Component Analysis (PCA) has been shown effective for reducing thermographic NDE data. A typical implementation of PCA is when the eigenvectors are generated from the data set being analyzed. Although it is a powerful tool for enhancing the visibility of defects in thermal data, PCA can be computationally intense and time consuming when applied to the large data sets typical in thermography. Additionally, PCA can experience problems when very large defects are present (defects that dominate the field-of-view), since the calculation of the eigenvectors is now governed by the presence of the defect, not the "good" material. To increase the processing speed and to minimize the negative effects of large defects, an alternative method of PCA is being pursued where a fixed set of eigenvectors, generated from an analytic model of the thermal response of the material under examination, is used to process the thermal data from the RCC materials.

Details of a one-dimensional analytic model and a two-dimensional finite-element model will be presented. An overview of the PCA process as well as a quantitative signal-to-noise comparison of the results of performing both embodiments of PCA on thermographic data from various RCC specimens will be shown. Finally, a number of different applications of this technology to various RCC components will be presented.

1. EXPERIMENTAL SETUP

For application to RCC materials, NASA is currently using the commercial infrared thermography system EchoTherm® manufactured by Thermal Wave Imaging, Inc. The IR imager is a commercial radiometer with a cooled 256H x 320V-element InSb (Indium - Antimonide) focal plane array detector. The radiometer's noise equivalent temperature difference (NEΔT), cited by the manufacturer, is 0.025°C when operating the detector in the 3 to 5 micrometer wavelength range. The radiometer produces images at both 30 frames per second output (video frame rate, in an RS170, format compatible with standard video equipment) and 60 frames per second output in a 14-bit, RS422 digital format. External optics, consisting of a wide-angle lens, using germanium optical elements, were used to increase the system field-of-view by a factor of approximately two. The expanded field-of-view of this lens is 41º horizontally and 31º vertically. Heat application is achieved by directing the output of two 4800 Joule xenon flash lamps contained within a hood assembly. The hood assembly helps to focus the energy onto the inspection surface.

Quantitative time based analysis requires synchronization between the IR imager and the heat source. This synchronization is achieved by computer control of the application of heat and the data acquisition. All experiments performed on the RCC material consisted of flash heating and then thermal data was acquired during the cool-down of the inspection area for a total of 14 seconds. Images were recorded at a frame rate of 60 frames per second. The camera/hood assembly was mounted on a photographic copy stand in order to maintain a consistent standoff of 2.54cm between the hood and the surface. For all cases presented in this paper, the maximum surface temperature change of the specimen above ambient was less than 10°C.

2. ONE-DIMENSIONAL ANALYTIC MODEL

To simulate the front surface temperature response of the RCC material to a flash heat input, a one dimensional, multi-layer model was developed to solve the heat equation. A classic Laplace transformation approach was taken to solve the heat equation[1,2]. The heat equation in a one dimensional slab of finite thickness is:

$$\frac{\partial^2 T}{\partial x^2} = \frac{1}{\alpha}\frac{\partial T}{\partial t} \qquad (1)$$

where T is temperature, t is time, x is the dimension normal to the surface of the slab with x=0 being the slab face of interest and α is the thermal diffusivity. The heat flux, Φ, is assumed for this model to be a Dirac heat pulse of total energy Q and is applied at x=0 with an insulating back surface (x = d) where d is the thickness of the layer. In the time domain this leads to the following boundary conditions:

$$\Phi = Q\delta(t) \quad \text{at x = 0 and,} \tag{2}$$

$$\Phi = 0 \quad \text{at x = d.} \tag{3}$$

Applying a Laplace transform to the heat equation yields:

$$\frac{d^2\theta}{dx^2} = \frac{P}{\alpha}\theta, \tag{4}$$

where P is the Laplace parameter and θ is given by:

$$\theta = \int_0^\infty e^{-Pt} T dt\,. \tag{5}$$

The boundary conditions can also be transformed into the Laplace domain as:

$$\phi = Q \quad \text{at x = 0 and} \tag{6}$$

$$\phi = 0 \quad \text{at x = d.} \tag{7}$$

It is typical to write the four quantities of interest θ_i, ϕ_i, θ_o, and ϕ_o, the front face Laplace temperature and flux and the Laplace temperature and flux at x = d respectively, in matrix form as:

$$\begin{bmatrix} \theta_o \\ \phi_o \end{bmatrix} = \begin{bmatrix} A & B \\ C & D \end{bmatrix} \begin{bmatrix} \theta_i \\ \phi_i \end{bmatrix}, \tag{8}$$

where,

$$\begin{bmatrix} A & B \\ C & D \end{bmatrix} = \begin{bmatrix} \cosh(kd) & \frac{1}{kQ}\sinh(kd) \\ Qk\sinh(kd) & \cosh(kd) \end{bmatrix}, \tag{9}$$

and

$$k = \sqrt{P/\alpha}\,. \tag{10}$$

Finally, a material of n layers can be expressed in matrix form, in the Laplace domain, as follows:

$$\begin{bmatrix} \theta_o \\ \phi_o \end{bmatrix} = \begin{bmatrix} 1 & -R_{n+1} \\ 0 & 1 \end{bmatrix} \begin{bmatrix} A_n & B_n \\ C_n & D_n \end{bmatrix} \begin{bmatrix} 1 & -R_n \\ 0 & 1 \end{bmatrix} \cdots \begin{bmatrix} A_1 & B_1 \\ C_1 & D_1 \end{bmatrix} \begin{bmatrix} 1 & -R_1 \\ 0 & 1 \end{bmatrix} \begin{bmatrix} \theta_i \\ \phi_i \end{bmatrix} \tag{11}$$

where R_n is a contact resistance that can be added between any layer to simulate a defect such as an air gap that would reduce the rate of heat flow. Once the matrix has been established, then numeric methods were used to perform the inverse Laplace transform back into the time domain.

The RCC material used on the Space Shuttle is actually a layered structure consisting of Silicon Carbide (SiC) on the front and back surfaces and reinforced carbon-carbon in the middle. Additionally, most specimens have other coatings of various types applied to the outer (front) surface. Because of the nonuniformity of the SiC layer as well as the complex nature of this material a four layer model was chosen to approximate the thermal response. A unitary input heat flux (Q) was chosen for the model since the actual heat deposited on the front surface is unknown.

Figure 1 shows the front surface temperature as predicted by the analytic model compared to experimental data for 15 seconds of cooling after the initial heat pulse for undamaged RCC material and for a flat-bottom hole 1.27cm in diameter with 50% of the material removed. The output of the model and the experimental results were both normalized for comparison. **Figure 2** shows the difference between the model and the experimental data, in the undamaged RCC case, as a function of time, indicating that agreement of better than 99% is achieved after 0.13 seconds of cooling. The difference observed over the flat-bottom hole can be partially attributed to a failure of the 1-D model to correctly account for two dimensional heat flow effects due to the presence of the defects and indistinct nature of the layers in the actual RCC material.

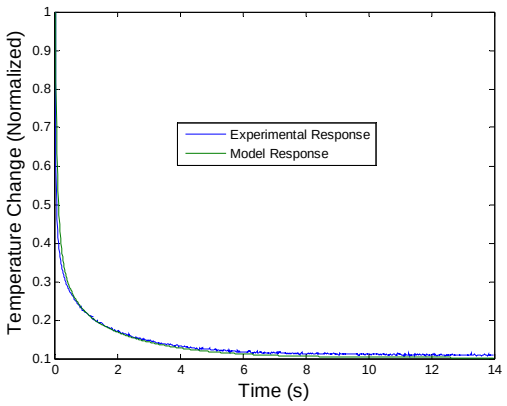

(a)

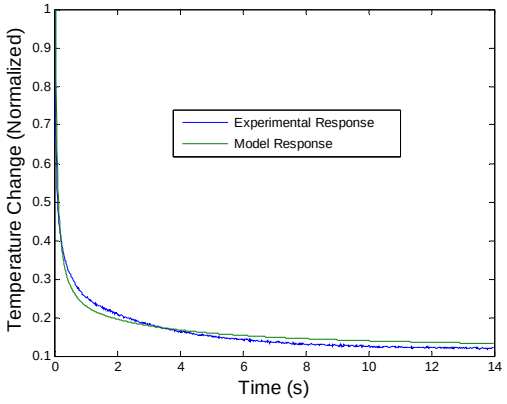

(b)

Figure 1. Comparison of four layer 1-D analytic model results with the experimental response of RCC material for two situations (a) no defect and (b) a flat-bottom hole.

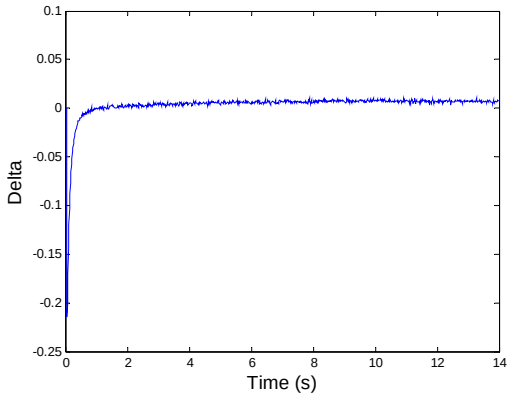

Figure 2. Difference between experimental results and analytic model of undamaged RCC material showing better than 99% agreement after 0.13 seconds.

3. TWO-DIMENSIONAL FEM MODEL

In order to further understand the response of the RCC material and to confirm the one-dimensional model results, a two-dimensional finite element model was developed using the commercial package FEMLAB®. The total width of the model was 15.24 cm. Three flat-bottom hole defects were also modeled with depths of 18.4%, 36.75% and 55.2% of the total material thickness. The model had 2991 total elements, 723 boundary elements and 6276 degrees of freedom. An insulating boundary condition was applied to all free surfaces except the top where inward convective flux was applied for 0.015 seconds (to simulate flash heating) and then replaced with convective cooling for the next 15 seconds, with time steps of 0.033 seconds. **Figure 3** shows a comparison of the FEM model with experimental thermal data for the case where no material loss is present and where 36.75% of the material has been removed. Generally good agreement between the model and the experimental data can be observed. The difference observed over the flat-bottom hole can be partially attributed to a failure of the FEM model to correctly account for convective losses. In this particular case the FEM model used a constant negative flux for convection losses instead of a temperature dependant flux.

4. PRINCIPAL COMPONENT ANALYSIS

PCA is a common data reduction methodology applied to thermal NDE data. The algorithm is based on the decomposition of the thermal data into its principal components or eigenvectors using singular value decomposition (SVD).[3-5] PCA is performed by first reformatting the three-dimensional thermal data into a two-dimensional array where the columns contain the spatial information and the rows contain the temporal information such that T(x,y,t) becomes A(n,m) where n = N_x * N_y and m = N_t. The matrix A is then adjusted by subtracting the mean along the time dimension, and decomposed to yield the eigenvalues and eigenvectors:

$$A = U\Gamma V^T \tag{12}$$

where U and V are orthogonal matrices who's columns form the eigenvectors of AA^T and A^TA respectively and Γ contains the singular values (the nonnegative square roots of the eigenvalues) of A^TA. Since the column of U corresponding to nonzero singular values form an orthogonal basis for the range space of A, the entire thermal data set can be described by this basis. Because thermal NDE signals are well behaved and slowly varying in time, the predominant temporal variations of the entire data set are usually contained in the first or second eigenvector. The PCA images are formed by calculating the dot product of the measured temperature response, pixel by pixel, with the eigenvectors of interest (usually the two associated with the largest eigenvalues).

Defects in RCC material change the local temporal variation of the data and thus appear as either light or dark regions in the PCA images.

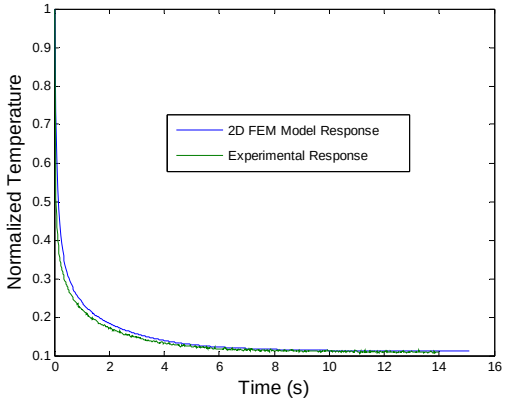

(a)

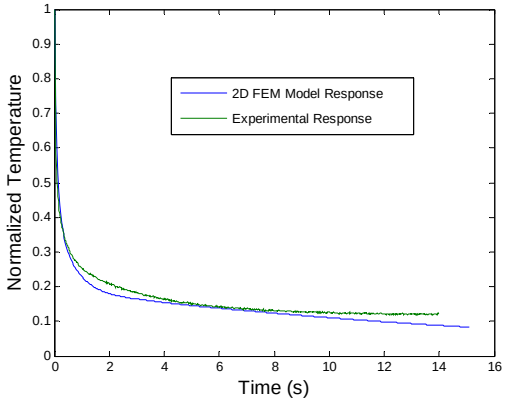

(b)

Figure 3. Results of the 2-D FEM Model for (a) RCC material with no defect and (b) a flat bottom hole with 36.75% of the material removed. Both cases are compared with experimental data.

While this process is quite effective in reducing thermal data, the SVD can be computationally intense especially with the very large three-dimensional arrays of thermal data typically produced in the inspection of RCC. In order to reduce the computation time involved, the results of the one-dimensional model of the RCC material with no defects was used to form the orthogonal basis. To provide a statistically rich data set for the calculation of the eigenvectors, a family of 10,000 characteristic curves were produced using the one-dimensional model. The curves represent a series of thickness variations of ±10% for each of the first three layers of the model. The resulting basis can then be used with any thermal inspection data to quickly form PCA images as described above.

5. EXPERIMENTAL RESULTS

A 15 cm square RCC specimen with 18 flat-bottom holes at five varying diameters and depths was used to compare the processing results of the two embodiments of PCA processing.

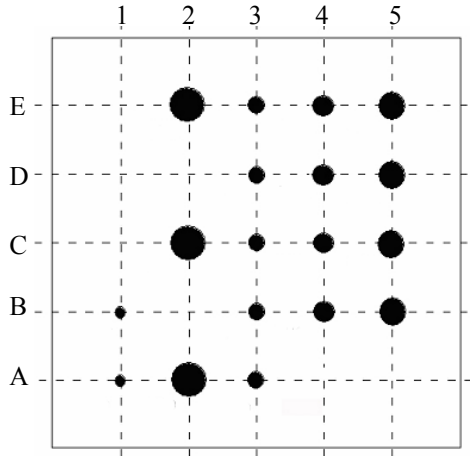

(a)

Row Number	Depth of Flaw
A	88%
B	72%
C	48%
D	24%
E	12%
Column Number	**Diameter of Flaw**
1	0.318 cm
2	1.27 cm
3	0.635 cm
4	0.476 cm
5	0.953 cm

(b)

Figure 4. Drawing of RCC flat-bottom hole specimen (a) and table of flaw diameters and flaw depths as a percentage of the total specimen thickness.

Figure 4 illustrates the size, depth, and location of the holes as observed from the back side of the sample. The depths of the defects ranged from material loss only in the silicon carbide layer (row E in **Figure 4a**) to holes 75% through the full thickness of the sample (row A). Flash thermography was performed on this specimen using the EchoTherm® system. Data was collected at a frame rate of 60 frames per second for 14 seconds after the flash heating. The data was processed using both conventional PCA and the fixed eigenvector PCA methods. **Figure 5** shows the results produced by the second eigenvector when applied to a time window of 0.167 to 3.5 seconds after heating. This time window is typically used to show defects close to the front surface of the specimen. **Figure 6** shows the results produced by the second eigenvector when applied to a time window of 1 to 11.5 seconds after heating, typically used for deep defect detection. Qualitatively the images look comparable, although the one dimensional model image appears to be slightly noiser.

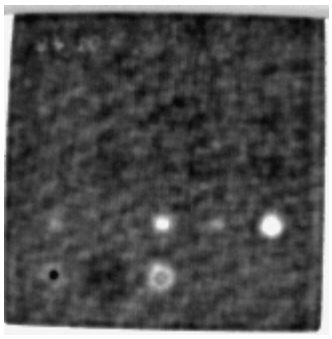

(a)

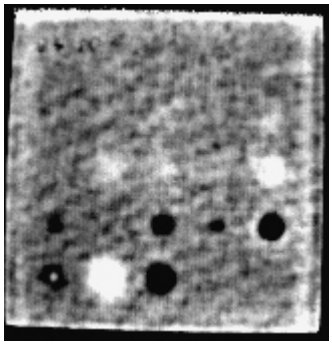

(b)

Figure 5. Second projection of early time window PCA images of RCC flat-bottom hole specimen processed with (a) conventional PCA and (b) fixed eigenvectors based on the one dimensional model.

To quantitatively compare the results of the model based eigenvector approach with conventional PCA the signal-to-noise ratio (SNR) was calculated for each of the 18 defects in both the early and late time windows. The average signal over a 3x3 pixel area in the center of each flat-bottom hole was used for the SNR calculation. Next, the average signal over a circle of 2.54cm in diameter around each defect was used as the background for the SNR calculation. The SNR was then determined from the following equation:

$$SNR = \frac{S^{defect} - S^{background}}{\sigma^{background}} \qquad (13)$$

where S represents the average pixel value and σ represents the standard deviation of the pixel values.

In general it can be seen from **Table 1**, which compares the two PCA techniques, that greater signal-to-noise ratios are obtainable using the model based fixed eigenvector PCA approach. This is especially true for the deeper defects such as E2, E3, D3, E4 and E5, where the fixed eigenvector approach brought the SNR above 1.0. The SNRs shown in **Table 1** are the largest values obtained by either technique, for either time window at each defect location.

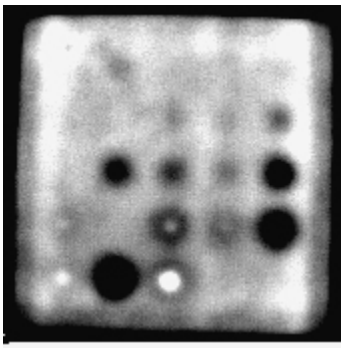

(a)

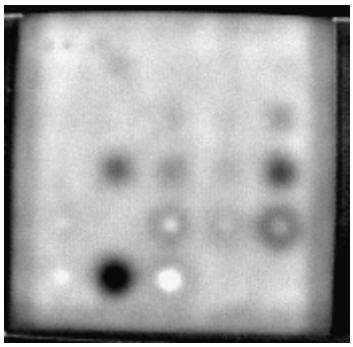

(b)

Figure 6. Second projection late time window PCA images of RCC flat-bottom hole specimen processed with (a) conventional PCA and (b) fixed eigenvectors based on the one dimensional model.

The fixed eigenvector approach was applied to thermal inspection data from the impact testing of RCC wing leading edge panels performed at Southwest Research Institute San Antonio, TX. **Figure 7a** shows a single frame from a high speed video camera of an ice projectile striking the surface of an RCC panel and **Figure 7b** shows that there is no visible surface damage to the panel. The projectile was a cylinder of ice 2.2cm in diameter and 3.33cm in length weighing 11.8g. The projectile impacted the RCC surface at 408.25 m/s with an impact angle of 23.5º relative to the plane of the material. **Figure 8** show a photograph of thermography being performed on a panel while it is installed in the impact test fixture. **Figure 9** shows the results of applying the fixed eigenvector PCA technique to the theromgraphic data acquired on the panel. **Figure 9a** is a near surface first eigenvector projection image of the impact area that was produced by applying the PCA technique to the data in a time window of 0.167 to 3.5 seconds after flash heating. **Figure 9b** reveals deeper damage from the impact by using a time window of 1 to 11.5 seconds after heating to create the first eigenvector projection. In this case damage was shown to be present in two different layers of the material, one close to the impact surface and one deeper. The total damage area measured 11.7cm in width and 11.9cm in height.

Defect No.	Model Based PCA Max SNR	Conventional PCA Max SNR
B1	6.3867	2.4165
A1	2.5937	10.3391
E2	1.9813	0.2155
C2	6.7688	4.7612
A2	11.134	13.8615
E3	1.0056	0.8833
D3	2.4172	0.5044
C3	7.9868	2.5116
B3	11.0751	20.032
A3	11.9819	23.7523
E4	1.1182	0.3772
D4	4.767	1.2643
C4	7.9	3.0336
B4	7.5803	5.5433
E5	1.5343	1.0771
D5	3.3425	0.4911
C5	8.2382	8.5228
B5	6.1298	9.2124

Table 1. Maximum signal-to-noise ratios for the 18 defects of the RCC calibration specimen calculated from the model based fixed eigenvector PCA and conventional PCA.

6. CONCLUSIONS

A new approach to PCA processing of thermal NDE data has been presented that uses a fixed set of eigenvectors generated from a one dimensional analytic model of the thermal response of RCC material. Application of this approach to data acquired from a flat-bottom hole specimen showed that an increase in the signal-to-noise ratio of the resulting images can be achieved over conventional PCA. Further, this technique was found to reduce the processing time required to analyze typical thermal data sets. For a set of thermal data containing 850 frames, full PCA calculating two eigenvectors on one time window required on average 46.6 seconds in Matlab®. For the same size data set, using the fixed eigenvectors previously calculated from the one dimensional model, the processing time was reduced by a factor of approximately 2.2. This reduces the processing time per data set to 21.0 seconds. This decrease in processing time becomes significant when applied to a complete inspection of the wing leading edges of the Space Shuttle. It is currently estimated that 600 data sets will be required to cover both wings during a thermal inspection. The use of fixed eigenvectors will reduce the processing time for this data by approximately 4.25 hours.

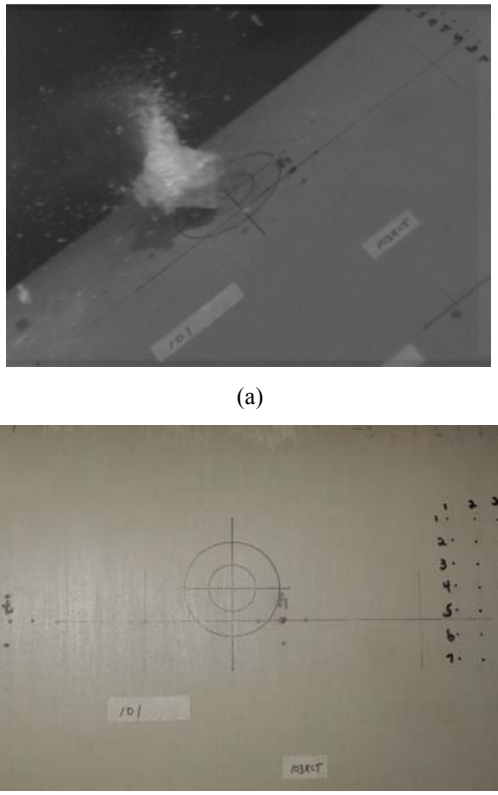

(a)

(b)

Figure 7. (a) High speed photograph of ice impact on RCC panel 9L-C and (b) a photograph of the target area after ice impact showing no visible indications of damage.

Figure 8. Photograph of thermographic inspection of RCC test panel after impact testing.

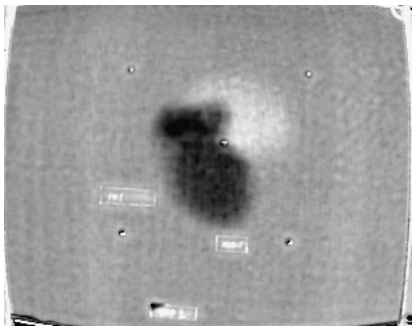

(a)

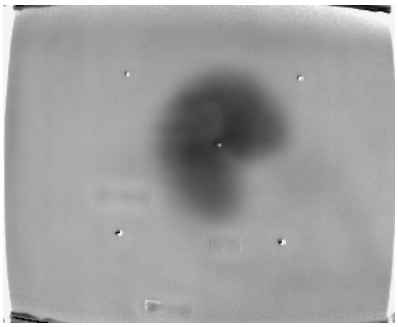

(b)

Figure 9. (a) Near surface and (b) deep PCA first eigenvector projections showing damage in RCC material from an ice projectile impact. The three rectangular and the five circular (half-light half-dark) indications are tape reference markers that were applied to the surface before thermography.

7. REFERENCES

1. H.S. Carslaw and J.C. Jaeger, *Conduction of Heat in Solids*, Clarenon Press, Oxford, 1986.
2. D. Maillet, et. al., *Thermal Quadrupoles*, John Wiley & Sons, Chichester, 2000.
3. N. Rajic, "Principal Component Thermography for Flaw Contrast Enhancement and Flaw Depth Characterisation in Composite Structures," Composite Structures, Vol. 58, pp 521-528, 2002.
4. N. Rajic "Principal Component Thermography," DSTO-TR-1298, 2002.
5. J.N. Zalameda, P.A. Howell and W.P. Winfree, "Compression Techniques for Improved Algorithm Computational Performance," Proceedings of SPIE, Thermosense XXVII, Vol. 5782, 2005, pp. 399-406.